Design, Development, and Characterization of a Flow Control Device for Dynamic Cooling Liquid-Cooled Servers

by

HARDIK YASHWANT HURNEKAR

Presented to the Faculty of the Graduate School of

The University of Texas at Arlington in Partial Fulfillment

Of the Requirements

For the Degree of

MASTER OF SCIENCE IN MECHANICAL ENGINEERING

THE UNIVERSITY OF TEXAS AT ARLINGTON

MAY 2021

Supervising Committee:

Dr. Dereje Agonafer
Dr. Abdolhossein Haji-Sheikh
Dr. Miguel Amaya

Acknowledgments

May 13, 2021

I would like to Thank Dr. Dereje Agonafer for his support and guidance he provided me throughout the time of my research in EMNSPC Lab. I would also like to thank him for helping me with my Thesis report and providing valuable tips for improving my work. I am extremely grateful towards him for presenting me with various opportunities to learn and understand the processes used in the electronic cooling field.

I would like to thank Dr. Amaya Miguel and Dr. Haji Sheikh for taking the time of their schedule and being a part of my thesis committee, providing me with their valuable guidance in improving my work.

I would like to thank Mr. Pardeep Shahi, Mr. Satyam Saini and Mr. Pratik Bansode for being my mentors and guiding me throughout my time at EMNSPC Lab and helping me to put up this report.

Lastly, I would like to thank my parents Mr. Yashwant Hurnekar and Mrs. Yashashree Hurnekar for believing in me and supporting me in every part of my life.

Abstract

Design, Development, and Characterization of a Flow Control Device for Dynamic Cooling Liquid-Cooled Servers

HARDIK YASHWANT HURNEKAR

The University of Texas at Arlington, 2021

Supervising Professor: Dereje Agonafer

Since the early ’60s, based on Moore’s law, transistor density has been doubling every generation resulting in increased power density. Eventually, in the early ’90s, we moved from constant voltage to constant electric field and corresponding constant power for a given area during technology changes. Dennard’s model of voltage scaling and corresponding constant power ceased, ending improved performance gains in the early 2000s that again required techniques to mitigate increased power and corresponding temperature. The performance gain is being achieved by using multi-core processors, leading to non-uniform power distribution and localized high temperatures making cooling very challenging. Direct cold plate-based liquid cooling is one of the most efficient cooling technologies. The servers in traditional liquid-cooled data centers operate at constant flow rates irrespective of the IT load on each server which leading to redundant pumping power. Dynamic cooling based on a new low-cost Flow control device (FCD) is designed to control the coolant flow rates at the server level. The dynamic cooling will result in pumping power savings by controlling the flow rates based on server utilization. The proposed FCD design contains a V-cut ball valve connected to a micro servo motor. The valve position is varied to

change the flow rate through the valve by servo motor actuation based on pre-decided rotational angles. FCD working was validated by varying flow rates and pressure drop across the device by varying the valve position using both CFD and experiments.

List of Illustrations

List of Tables

Table of Contents

Chapter 1

Introduction

In the modern age, computers have become the most important tool for almost all functions ranging from household use, machine operation to medical applications. With the rise of Artificial intelligence and machine learning the need for data storage and data processing has become more prominent. As of now, it can be said that data has become the new oil, and companies are developing and transforming technologies that can help them to process and store a large amount of data that is generated every day. The function of storing and processing the data is done by powerful computational devices called servers. The servers are equipped with high-power microprocessors capable of executing billions of operations per second at very high TDP (Thermal Design Power), as a server is an electronic device with components such as CPU and GPU and other power components operating at high TDP resulting in the production of heat. The highest operating temperature of Silicone chip is 125° C and longer exposure to these temperatures can lead to Reliability issues. To address this issue, heating components are needed to be cooled by the means of conduction, convection, and Radiation. Convection is the most effective type of heat transfer method. A fluid medium is blown over the Heated component to cool the components. To achieve efficient cooling the servers are housed in a dedicated space in a building called as a data center. Data centers have a controlled environment and protect the electronics from outside dust and moisture which can harm the electronics. Traditionally data centers are cooled using two methods:

1. Air cooling
2. Liquid cooling

1.1 Air cooling

Air cooling is the most prominent method used in data centers. More than 80% of IT companies are using Air cooling in their data centers, because of the simplicity in design and cost-effectiveness. Air cooling is half a century old technology, extensive research and development is available for this technology which drives its cost low and is a tried and tested method. In Air-cooled data centers, the servers are housed in a rack, a maximum of 42 servers can be fitted into one rack due to power consumption limitation. Each server has fans arranged in parallel or series depending on the resistance provided by the components in a server. The fans help in blowing air over the electronic components. Heatsinks are used to increases the area of heat transfer for high TDP components. The Racks Are placed on an elevated floor. A CRAC (computer room air conditioner) is used to supply cold air from the ducts below the floors the cold air enters the servers through suctions produced by fans and hot air is given out at the other side. The hot air rises through natural convection currents and it enters the CRAC unit where heat is exchanged with external fluid. The CARC is supplied cold fluid through Chillers. Studies suggest that traditional air-cooled data centers use approximately 30-40% of energy for cooling purposes [1-2]. With the drastic increase in heat flux in GPUs and CPU's air cooling is on the way to obsolescence. Studies suggest that the average High power usage effectiveness (PUE) is still around 1.58. The reason for this is inefficient cooling [3]. In coming years there will be a need of substituting traditionally used air cooling with more efficient methods such as liquid cooling and several other methods which will help in efficient heat transfer [4-6]. Figure 1. Shows schematic arrangement of traditional air-cooled data center.

.

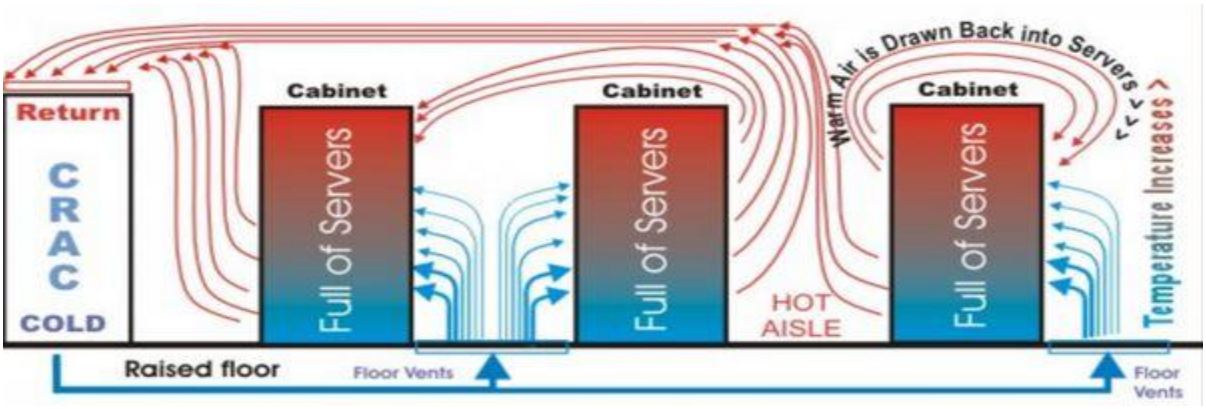

Figure 1. Schematics of a traditional Air-cooled Data Center

Source: colocation America website

1.2 Liquid cooling

DLC (Direct liquid cooling) is already in use and has proven to be a highly efficient solution to meet the ever-increasing cooling demand. DLC has already been used since 1960, but due to development in CMOS, air cooling once again become a viable option [7-10]. In modern times the need for higher power multicore CPU has increased, along with this the trends are again shifting towards liquid cooling [11-13]. In liquid cooling, the operating fluid is liquid which has high thermal conductivity and high thermal mass when compared to air. Heat sinks are replaced with cold plates shown in Figure (4), due to the high thermal conductance of fluid, heat transfer can take place at a reduced area when compared to heatsinks. The cold plate is supplied cooling fluid through the inlet manifold and the hot liquid exits from the cold plate to the outlet manifold. Both the inlet and outlet manifolds are connected to a CDU. The CDU houses the pump which supplies the liquid at required flowrates to the servers and it also acts as a heat exchanger. The hot fluid from the server exchange heat in the CDU with the external fluid supplied from the chiller which then exchanges the heat with the atmosphere. The advantage of DLC is that it can be

integrated in a hybrid manner where high-power components are cooled using cold plates and other components are cooled using airflow from the fans [14]. Other types of data centers use total liquid cooling by implementing cold rails for cooling other components like Memory sticks along with cold plates [15]. Figure (2) shows Schematics of a traditional liquid-cooled data center and Figure (3) shows the arrangement of placement of the cold plate assembly, in a traditional DLC data center, the cooling fluid is circulated at a constant flow rate irrespective of the utilization of the servers if the utilization of the server is taken into consideration and flow rates are varied according to significand saving in pumping power can be achieved.

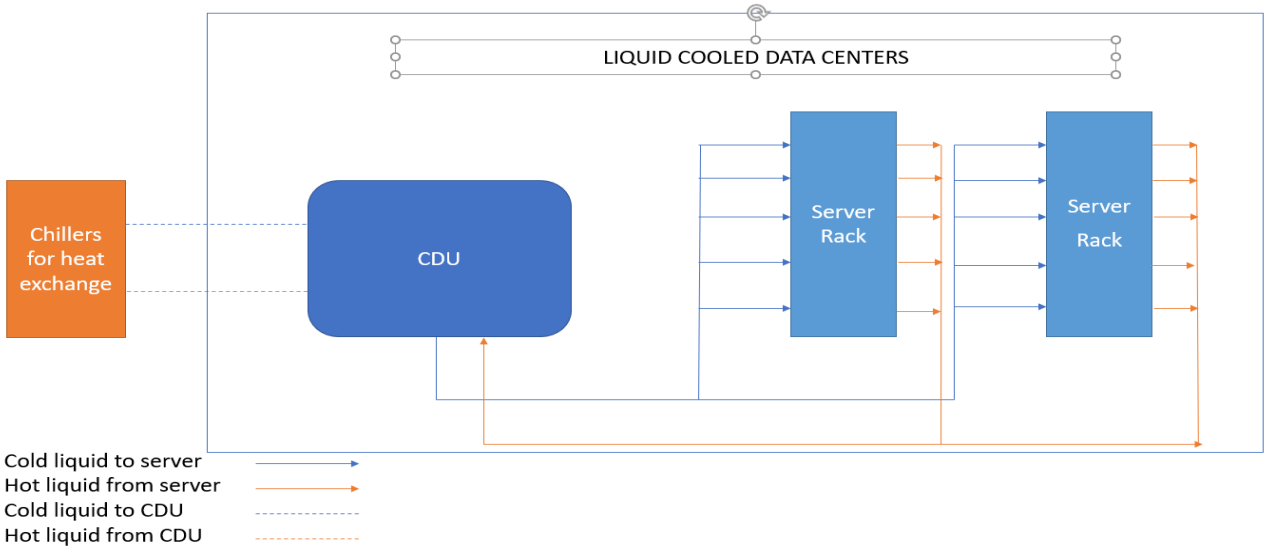

Figure 2. Schematics of a Liquid-cooled data center

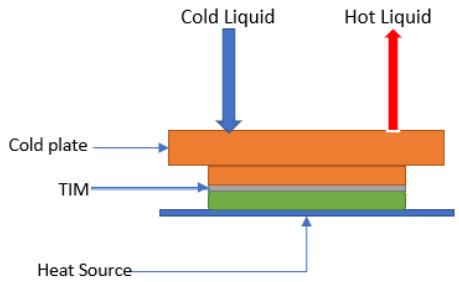

Figure 3. Schematic of placement of cold plate

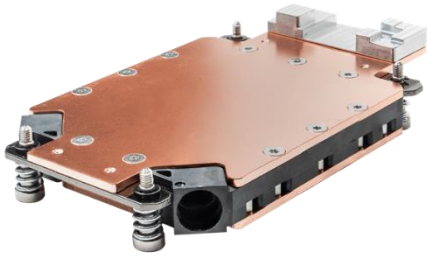

Figure 4. Image of cold Plate

Image source: Cool it Website.

Dynamic liquid cooling is one such method, In the past Dynamic cooling has been implemented in Air cooling method. An improvement of 70% in data center performance was observed by controlling The CRAC Fan speed and electronically actuating the air vents [16]. The process of dynamic cooling can be further improved by implementing automation of the process through machine learning, where the fan speed and the opening of vents can be controlled using the feedback from the sensors recording the temperatures on the heating components [17-21]. In Dynamic liquid cooling, similar results can be achieved by developing a control strategy and controlling the flow on each server using a flow obstruction device. A similar study was conducted by Kasukurthy in which a control strategy was developed for FCD and simulation was done using

CFD software, a pumping power saving of 64% was achieved [22,23]. The obstruction of flow can be achieved by developing a Flow control Device that can be implemented on each server in a data center at low manufacturing cost and high reliability and low cost to Reproduce the components.

In our study, we will go through the design, development, and validation of Flow characteristics of a Flow control Device that can be integrated with IT equipment for Dynamic variation of fluid flow rate based on the working load of the servers. The FCD is a V-cut ball valve. The Area of the opening of the valve is proportional to the angle of rotation of the valve. A servomotor is used as an actuator to rotate the damper. the variation in flow rate with respect to change in rotation angle of the valve. To validate variation in the flow rate and pressure drop across the device were analyzed by varying the position of the valve. Results obtained using Computational Fluid Dynamics and Experimentation were compared to validate the working of FCD.

The thesis is outlined in the following section: design and development of the FCD, CFD analysis of the final design, FEA analysis for the valve, and validation of the results for the proof of concept. Experimentation and comparing the results with the CFD result to confirm the working of the FCD.

Chapter 2

Design and Development of Flow control Device

2.1 Design Motivation

The primary motivation of the study is to design and develop a Flow control device that can be implemented in a Dynamic cooling setup. Experimentation on implementation of targeted delivery of flow have already been done in Air-cooled data centers, a reduction in energy expenditure for transportation of fluid was observed due to prevention of over-provisioning of fluid. The purpose of this study is to produce similar results in Dynamic liquid cooling by the implementation of a Flow controlled device. The FCD uses an actively controlled damper which is actuated using a servo motor. The position of the damper will decide the area of opening which controls the flow rates according to the utilization of the servers. This targeted control of Flow will result in pumping power saving in data centers, making the cooling process more efficient. The FCD is designed in such a way that it can be manufactured at a low cost using additive manufacturing techniques such as 3D printing. This makes the manufacturing process cost-efficient when produced on a large scale. Usage of additive manufacturing makes the design easy to reproduce.

2.2 Design and Development

The design and development of any product start with the market research and need of the product. The market research helps in specifying the engineering characteristics needed for products. In our case, the FCD needs to provide minimum flowrate at a closed position without shutting down the flow completely. The FCD should use materials that are strong enough to withstand the pressure at working conditions flowrates with high reliability and good cycle life.

The FCD developed are needed to be implemented in data centers with thousands of servers, hence mass production of these devices is needed at reduced manufacturing time and effective reduction in manufacturing cost.

2.2.1 Concept of Design

The next step for any designing process is generating several concepts and comparing the engineering characteristics of the concepts. In our case, two designs were taken into consideration, the Butterfly valve, and the V-cut ball valve. A prototype design of the Butterfly valve was made in CAD software shown in Figure (5) and was tested for variation in flow rates with change in angle using CFD Analysis. The results showed minor variation in flow rates with change in angle, but the variation in flow rate was not sufficient for our use. Hence the ball valve design was taken into consideration. Ball valves are frequently used in industries for On/Off purposes and cannot reproduce precise control over the flow. Recent development in V cut ball valve has shown significant improvement in the linear response and allows a wide range of flowrate [24,25]. With this conclusion, the V-cut ball valve was chosen and the CFD analysis resulted in the required characteristics and variation in flowrate with change in the damper angle. The illustration of conceptual design of V-cut ball valve is shown in Figure (6) Results from CFD analysis for both butterfly and V-cut ball valve are compared using graphical data and is shown in Figure (7).

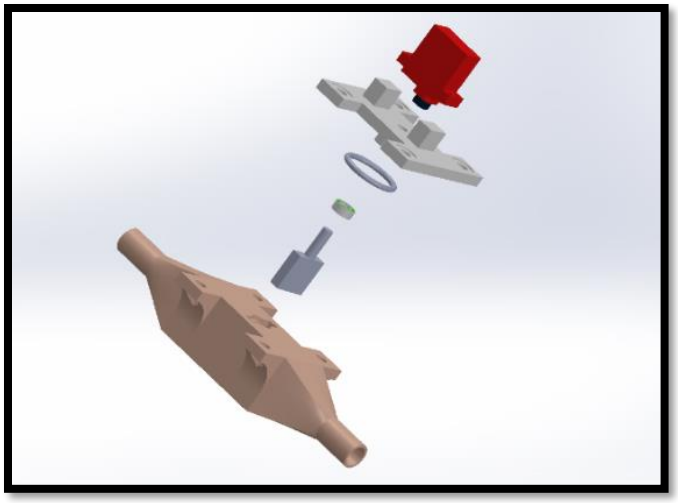

Figure 5. Conceptual design of a butterfly valve

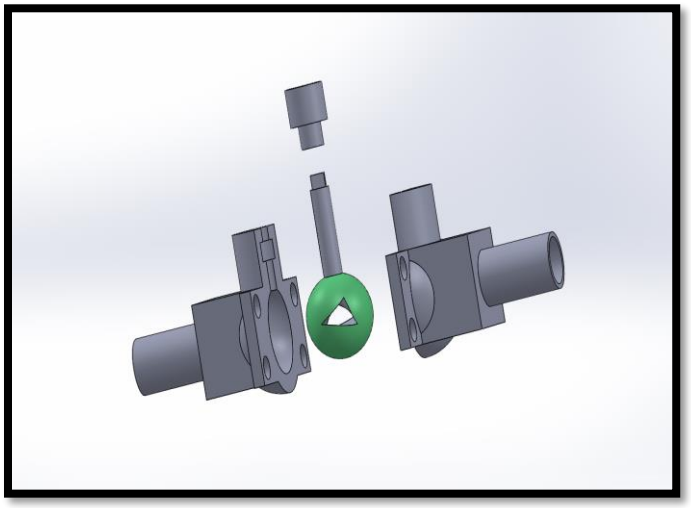

Figure 6. Conceptual design of a V-cut ball valve

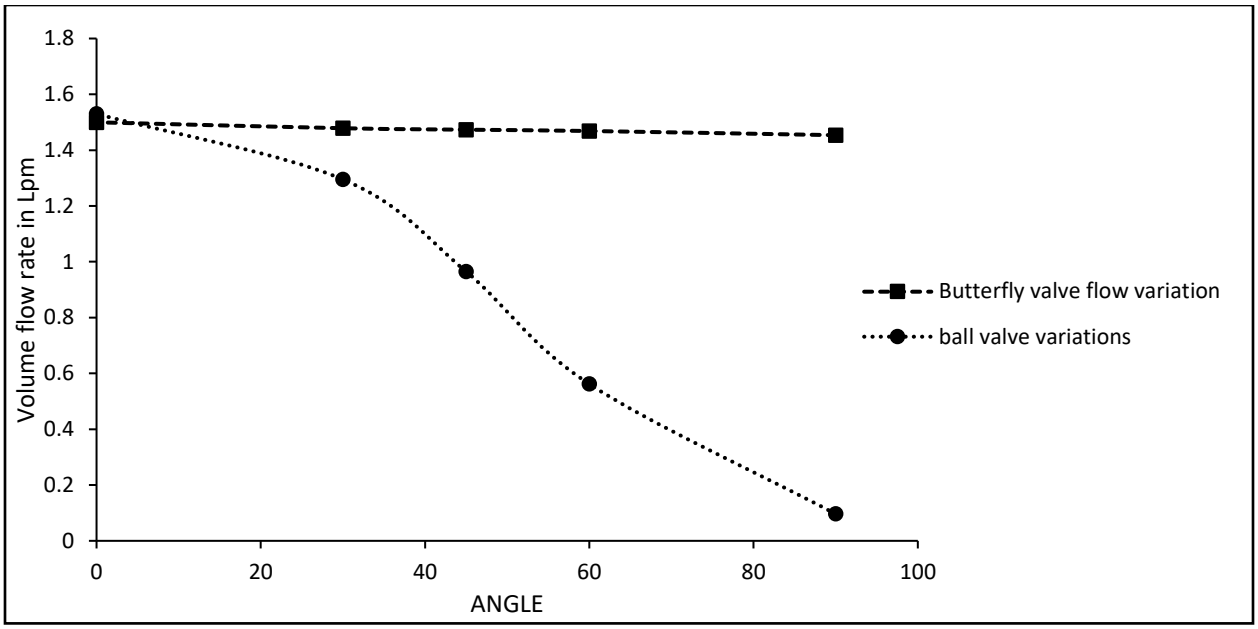

Figure 7. Comparison of flow rate variation between the V-cut ball valve and initial Butterfly valve

2.2.2 Detailed Design

Based on the comparison and validation of results obtained from the conceptual design Phase, a V-cut ball valve was chosen. A detailed design was drafted taking into consideration standard pipe size for Inlet and outlet, in our case the external diameter of the inlet and outlet pipe of the FCD was chosen to be 3/8 inches, and a 10 mm ball valve size was chosen. The shaft of the valve was 13mm in diameter and a standard shaft seal was chosen to prevent fluid leakage from the moving parts. The top of the shaft has grooves where the servomotor arms can be directly fitted. The Detailed design was drafted in SolidWorks keeping in mind the conditions needed to manufacture the part using additive manufacturing. Figure (8) shows a detailed exploded view of the FCD that is designed, and Figure (9) shows the final assembly. Manufacturing a part using 3D printing machines needs special design consideration which depends on the method of printing

and the ability of the machine hence. For our purpose, the FCD produced needed to be leak-proof, two methods of 3D printing were used.

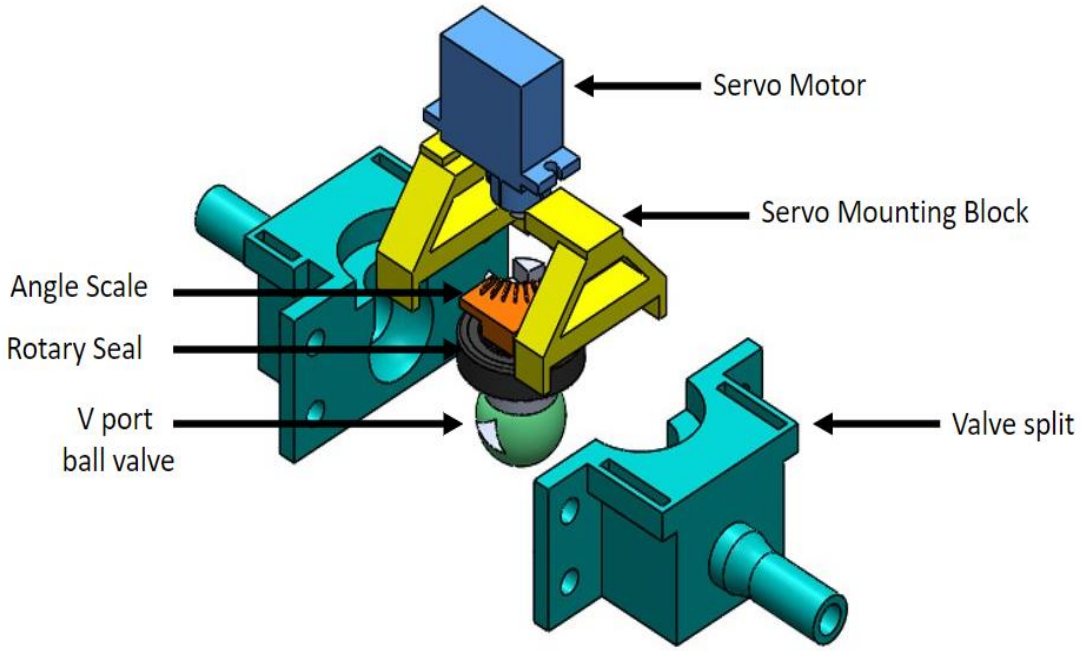

Figure 8. Exploded view of Flow control Device.

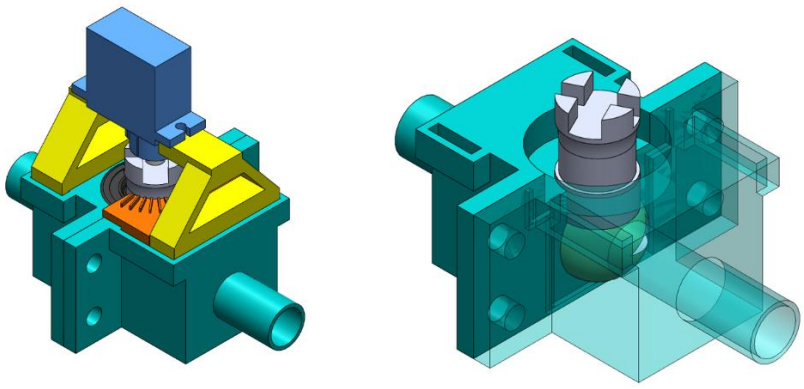

Figure 9. The above figures show the CAD Assembly of FCD

2.3 Manufacturing Method

The FCD developed should be cost-effective and easy to reproduce. By implementing additive manufacturing, we can cut the cost required for manpower and tooling. Additive manufacturing can produce complex geometries that are complicated to manufacture using traditional CNC machines. For the manufacturing, the FCD we tested two methods which are explained below.

2.3.1 Fused deposition modeling

Fused deposition modeling is one of the most common types of additive manufacturing techniques used. The machine Prints the component layer by layer with the layer plane perpendicular to Z-axis. Schematics of the FDM machine are shown in Figure (10). A common material used is PLA and ABS. the minimum thickness of the single layer is 0.125mm. even with 100% infill. There are voids in the structure which can lead to leakages and the surface finish is not as good as traditional manufacturing. FCD parts printed using FDM process are shown in Figure (10). It was observed that when the flowrate increased beyond 3 lpm the FCD started to leak from voids between the layers. Hence another method was needed which can result in a finer quality of print.

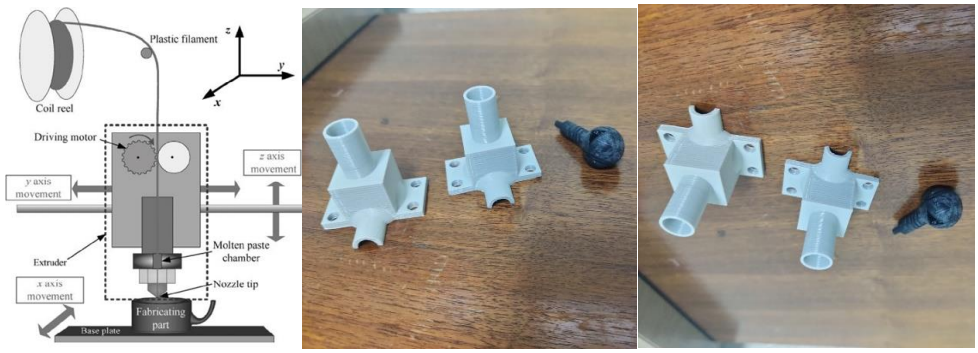

Figure 10. Schematic of FDM machine and FCD parts produced using FDM.[44]

2.3.2 HP MultiJet fusion printers

Additive manufacturing has come to such a stage that, some machines can reproduce parts with quality that are like parts produced using traditional manufacturing machines. One such machine is the HP MultiJet Fusion Printers, a good quality print was achieved with finer surface finish and no voids were generated during manufacturing. The FCD manufactured using this printer resulted in operation without leakage even at high flow rates. The print quality was similar to parts produced using traditional Machining. The material used is Nylon 66 which is suitable for high-pressure application and is not affected by the fluid's chemical properties. The material is used in powder form and unused powder can be reused from time to time. Figure (11) shows the HP MultiJet Fusion printer and the parts produced using the machine.

Figure 11. HP MultiJet Fusion printer and the FCD manufactured using this machine.

Chapter 3

Computational Analysis

Computational Analysis software such as ANSYS is an excellent tool for pre-production analysis of the model, it helps in identifying the required Engineering characteristics. These Analysis tools help predict the mechanical limits and cause of failure in the model. The results obtained using CFD analysis can be further validated with the experimental results. In our case, ANSYS Fluent was used for CFD calculations and ANSYS static structural was used for structural analysis of the model.

3.1 Computational Fluid Dynamics

Over the years CFD has become one of the most important tools for finding the characteristics and properties of the Flow in each system. For our purpose, ANSYS Fluent was used to conduct CFD analysis and to visualize the 3D flow inside the FCD. The CFD software uses momentum, energy, and mass conservation equation to solve the problem that is presented [26]. CFD analysis can be conducted on the CAD model that is generated using CAD software. Before preparing the setup for solving the model needs to be divided into small elements. This process is called meshing. A fine mesh helps in predicting accurate results. Before meshing is done the model generated is needed to be prepared for simulation. In our case only the hydraulic characteristics are needed to be studied, hence only the fluid domain is needed. A volume extract is created for the flow domain and other solid components are suppressed for physics. This helps in cutting off the extra efforts needed to mesh and solve the simulations.

3.1.1 Meshing

The mesh generated is a tetrahedral type of mesh for fast-paced calculations. The quality of the mesh is determined by the element skewness and the orthogonality of the mesh. For the mesh to be of good quality, the value of skewness should be closer to 0, and the value of orthogonality should be closer to 1. The minimum element size was set to be 0.3mm and the maximum element size was 0.6mm. the growth rate was 1.2 for the inflation and the number of layers in inflation was set to 10 layers. The average orthogonality of 0.8 and average skewness of 0.2 were observed in our case. Mesh independence study was carried out and it was found that the optimum number of elements count was 739,416. After creating the required mesh, the next process was setting up the CFD setup.

3.1.2 CFD setup

The main purpose of the CFD simulation was hydraulic verification of the FCD. The energy equation was deactivated which results in the deactivation of any Thermal inputs possible in the simulation saving considerable time required for solving the analysis. A pressure-based solver algorithm was used to simulate a velocity field through the FCD by a correction in the pressure equation in the continuity equation. During the literature survey, it was seen that various turbulence models were used for these types of flow applications. Literature shows that the $k-\omega$ turbulence model is most preferred. In our case, the Standard and Shear Stress Transport (SST) $k-\omega$ turbulence model was used because of its superiority in predicting such flow [27]. The SST $k-\omega$ model can predict the values of the drag coefficient across the fluid field. This has been validated in the literature where several turbulent models were solved for the butterfly valve design [28]. The CFD results become less sensitive to grid size when using this turbulence model.

The governing equation which controls the working of the simulation are given below.

Continuity equation:

$$\frac{\partial \rho}{\partial t} + \nabla.(\rho u) = Sm \tag{1}$$

Momentum:

$$\frac{\rho d\vec{u}}{dt} = -\nabla p + \nabla \cdot (\mu \nabla \vec{u}) + \vec{f} \tag{2}$$

Transport Equation for the SST $k - \omega$:

$$\frac{\partial}{\partial t}(\rho k) + \frac{\partial}{\partial x_i}(\rho k u_i) = \frac{\partial}{\partial x_j}\left(\frac{\partial k}{\partial x_j}(\mathrm{r}_k)\right) + \tilde{G}_k - Y_k + S_k \tag{3}$$

$$\frac{\partial}{\partial t}(\rho \omega) + \frac{\partial}{\partial x_i}(\rho \omega u_i) = \frac{\partial}{\partial x_j}\left(\frac{\partial \omega}{\partial x_j}(\mathrm{r}_\omega)\right) + G_\omega - Y_\omega + D_\omega + S_\omega \tag{4}$$

equations (3) and (4), $\tilde{G}_k$ represents the generation of turbulence kinetic energy due to mean velocity gradients, G_ω represents the generation of ω. r_k andr_ω represent the effective diffusivity of k and ω, respectively. Y_k and Y_ω represent the dissipation of k and ω due to turbulence and D_ω represents the cross-diffusion term. S_k and S_ω are user-defined source terms which were not utilized in the current CFD modeling setup [26].

After the turbulence model was selected, material properties were defined for the fluid. 25% Propylene glycol (PG25) is used as the fluid. In the boundary condition, the inlet of the FCD was set as inlet velocity. The outlet of the FCD was set to outflow with 0pa gauge pressure. The walls of the Fluid domain were treated as adiabatic walls and a steady-state solver was used with convergence criteria of $1*10^{-3}$ for velocities, continuity, k and ω values. Figure (12) shows the boundary conditions applied in the CFD setup.

Similar steps of meshing, setup of analysis was repeated for different cases by changing the damper handle from 0^o-90^o angle.

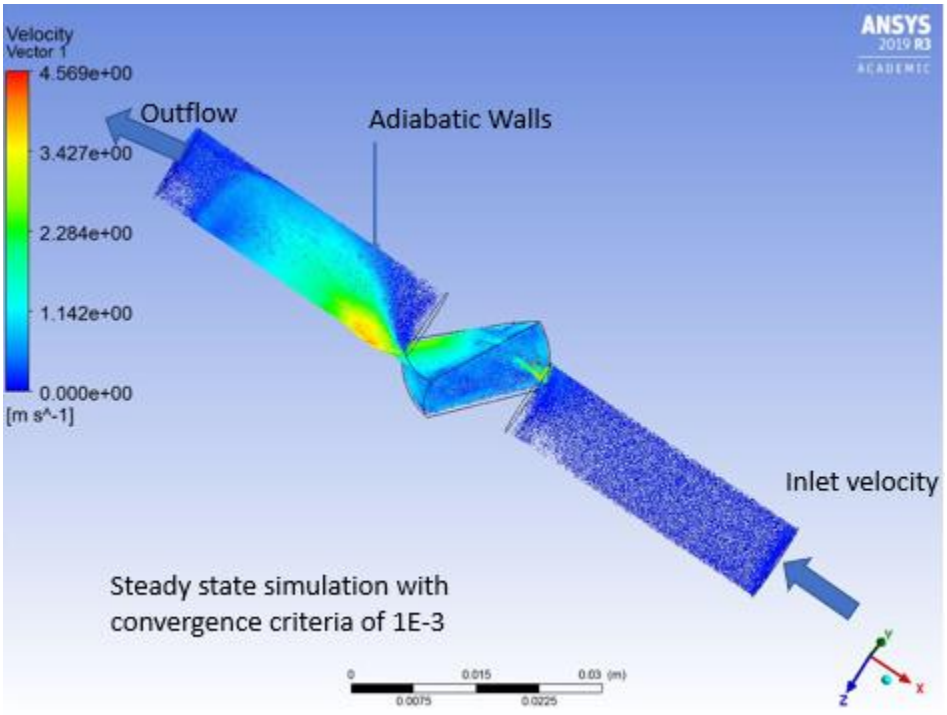

Figure 12. Boundary conditions for the CFD setup

3.1.3 CFD Result

After the convergence was achieved with the appropriate mesh, the CFD results were obtained and analyzed in the form of pressure drop across the FCD with change in the damper angle. The CFD simulation for 0^o,30^o,45^o,90^o was repeated for three chosen values of starting flowrate of 0.6, 1.0 and 1.5lpm. The CFD proved the working of the FCD, it was observed that with change in damper angle the pressure drop increases and the flow rate decreases. These results will be used to compare with the experimental results. The observation obtained showed similar trends when represented graphically for all the simulations. The values had error possibilities of 14%. Table.1, Table.2, Table.3 represents the pressure drop and flow rate values obtained during

the CFD analysis at starting LPM of 0.6, 1 and 1.5, respectively. Where Lpm stands for Liters per minute of flow and kPa stands for Kilo Pascal of Pressure. The data from the tables show that as the angle increases from 0^o to 90^o, the flow rate drops down to near 0 and the pressure drop increases from the minimum value. Figure (13), Figure (14) and Figure (15) shows the hydraulic characteristics of the FCD at fully open, partially open and at about to close position.

At 0.6 Lpm @ fully open				
v=0.127 m/s	**Inlet Pressure (kPa)**	**Outlet pressure (kPa)**	**Flow Rate (Lpm)**	**Pressure drop in (kPa)**
Angle				
0	6.23	5.154	0.725	1.076
30	6.013	3.985	0.625	2.228
45	4.256	0.765	0.412	3.491
90	9.286	1.896	0	7.39

Table 1.CFD Result showing increases in pressure drop with increase in damper angle at Maximum of 0.6 Lpm.

At 1 Lpm @ fully open				
v=0.2122 m/s	**Inlet Pressure (kPa)**	**Outlet pressure (kPa)**	**Flow Rate (Lpm)**	**Pressure drop in (kPa)**
Angle				
0	11.9856	10.456	1.19	1.5296
30	12.465	9.125	0.865	3.34
45	17.839	4.265	0.512	13.574
90	18.563	2.663	0	15.9

Table 2. CFD Result showing increases in pressure drop with increase in damper angle at Maximum of 1 Lpm.

At 1.5 Lpm @ fully open				
v=0.318 m/s	**Inlet Pressure (kPa)**	**Outlet pressure (kPa)**	**Flow Rate (Lpm)**	**Pressure drop in (kPa)**
Angle				
0	22.645	20.01	1.53	2.635
30	25.126	18.256	1.395	6.87
45	28.3692	9.564	0.965	18.8052
90	30.827	3.693	0.0964	27.134

Table 3. CFD Result showing increases in pressure drop with increase in damper angle at Maximum of 1.5 Lpm.

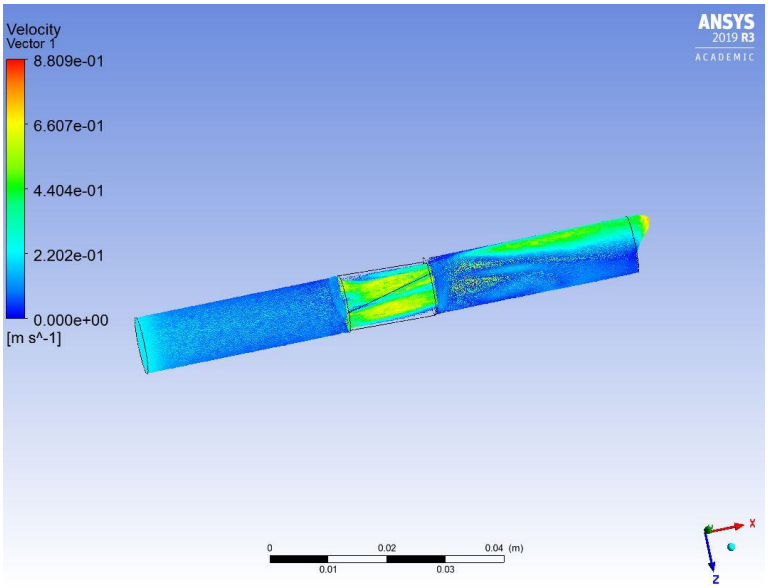

Figure 13. Flow characteristics when the valve is fully open.

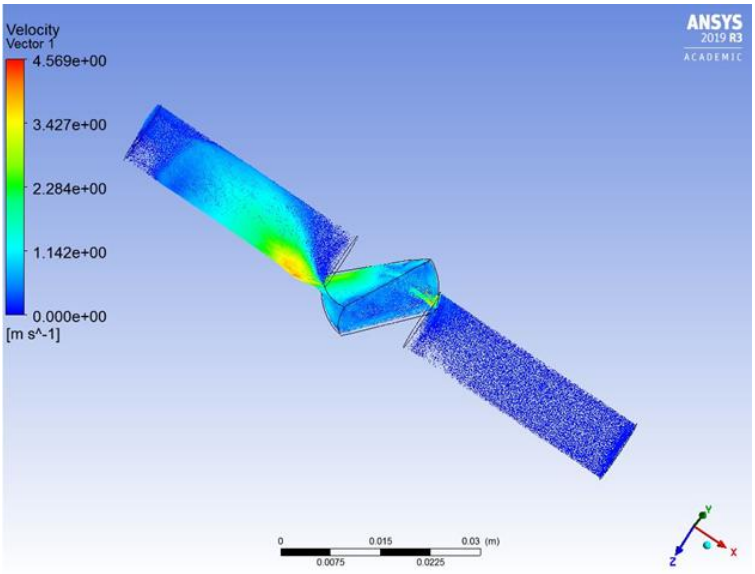

Figure 14. Flow characteristics when the valve is closed at 45 degrees.

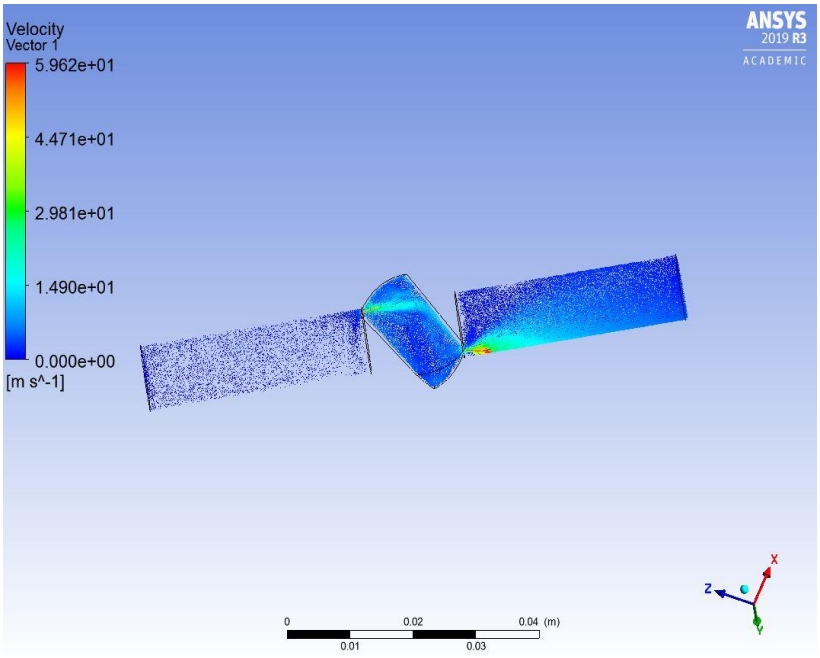

Figure 15. Flow characteristics when the valve is about to close.

3.2 FEA Simulations

The FEA solution was done using Static structural on Ansys workbench to test the working limit of the FCD. The internal load like pressure on the inner surface of the FCD was imported from the results of the CFD simulation. A tetrahedral mesh was used with a physical preference set to mechanical for calculating mechanical characteristics. The mesh element size was set to 0.5mm. the mesh smoothing was set to medium, the mesh resulted in 912689 nodes and 534030 mesh elements. The ambient temperature of the simulation was set to 22 C. Fixed support boundary condition was given to the sidewalls and loads were imported from the CFD simulation at highest flowrates at 4 Lpm. The basic assumptions in this theory include a linear elastic behavior and small deflections of the material.

$$[K]\{x\} = \{F\} \qquad (5)$$

Here [K] represents the stiffness matrix of the entire geometry. {x} represents the unknown nodal displacements and {F} represents the external forces or applied loads.

3.2.1 FEA Results

It was observed that the maximum deformation was observed near the inlet port where the pressure is high. With a value of 7.9e-04 mm with maximum equivalent stress of 0.94 MPa. The average deformation observed throughout the FCD was 1.13e-04 with average stress of 7.6e-02 MPa. The average factor of safety observed was 15, the above results are shown in the Figure (16), Figure (17), Figure (18), hence it can be concluded that the current dimension and material will not fail at high-pressure conditions observed at a maximum flow rate of 4 Lpm. To further validate the results observed in the CFD and FEA analysis experimentation is needed to be done to get real working values.

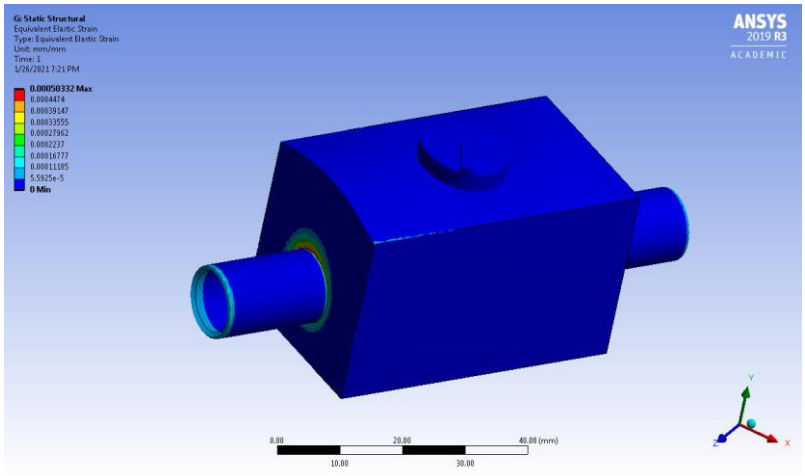

Figure 16. Equivalent Elastic Strain

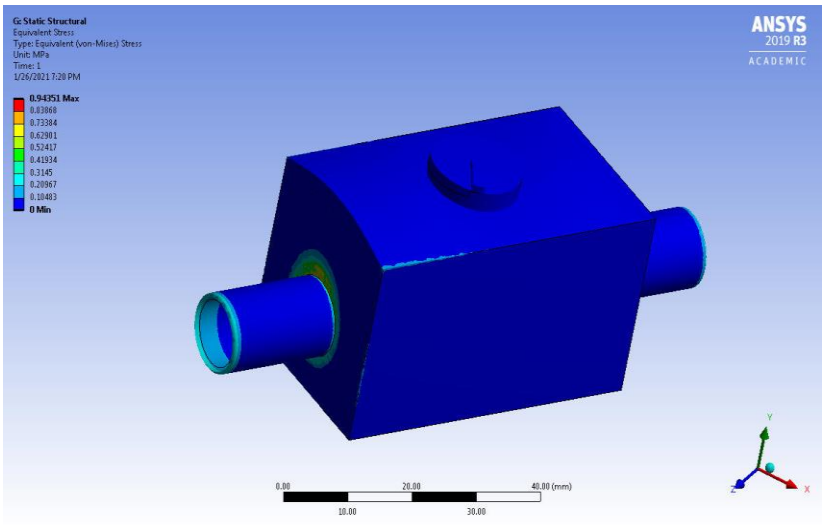

Figure 17. Equivalent (Von-Mises) Stress

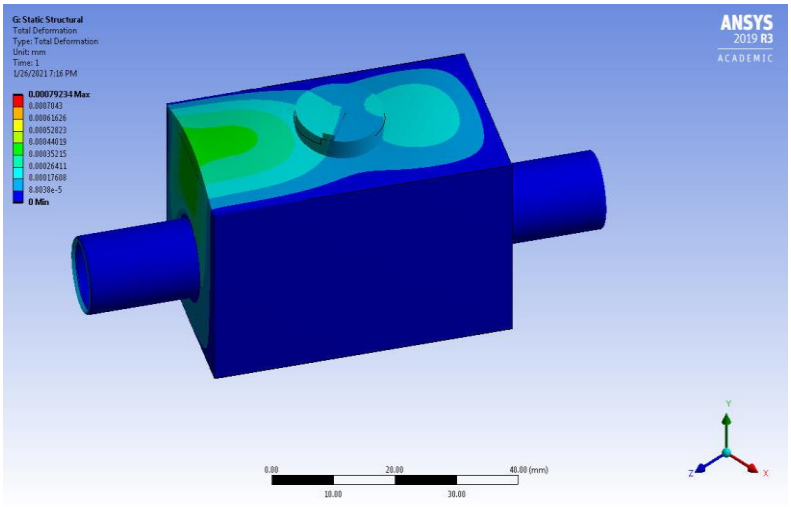

Figure 18. Total Deformation

Chapter 4

Experimentation

An experiment was carried out in a temperature-controlled environment where the ambient temperature was set to 22^{o} C. the Fluid used for circulation is PG 25, and a closed-loop experimental setup was built around the FCD to prevent contamination of the fluid. Two pressure sensors were attached at the inlet and the outlet of the flow control device. To determine the pressure, drop in the FCD. An ultrasonic flowmeter was used to calculate the flow rate. the ultrasonic flow sensor works on the principle of the doppler effect which finds the value of the flow rate of the fluid depending on the Hydraulic diameter of the pipe and velocity of the fluid. The Ultrasonic flow meter and the Pressure sensor were connected to the Data acquisition system (DAQ) which is used for sampling electric signal. The pressure sensor and the ultrasonic sensors generate an electric current that is linearly proportional to the value of pressure or flow. The DAQ converts these electric signals into Known units such as Pressure in pascals and flowrate in Liters per minute. The pressure sensors and the ultrasonic flowmeter need external power, 20V was given using an external DC power supply. A PWM-controlled pump running at maximum of 15 Watts of power was used to circulate the fluid in the loop. The speed of the pump is controlled by the value of PWM supplied by the microcontroller which is preprogrammed for this purpose. By controlling the speed of the pump, we can control the Flowrate in the experimental setup loop. The angle of the valve was controlled using a servomotor attached to the shaft of the flow control device. An Arduino microcontroller was used to control the valve opening.

The Arduino was programmed using Arduino Ide and the angle of the servo motor depended on the value of the resistance provided by the Potentiometer. The experiment was

conducted at a minimum of 0.2 Lpm and a maximum of 4 Lpm of starting Lpm. Observations were notated at 0^{o}-90^{o} angle. The schematic of the experimental setup is shown in Figure (19).

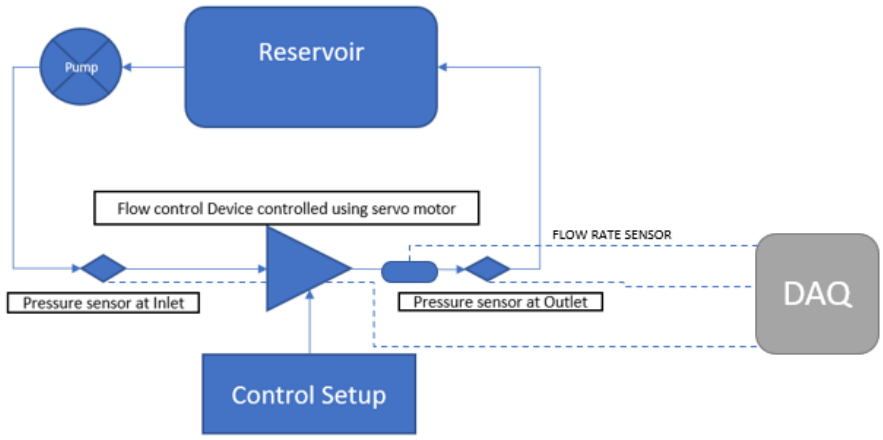

Figure 19. Schematic of the experimental setup used for characterizing the flow control device.

4.1 Experimental Result

After the CFD simulation and proof of working observed from the CFD and the FEA results. Experimentation was conducted with a starting of 0.2 Lpm and a maximum starting was4.0LPm. Results from the Experiment are represented in the graphical format shown in Figure (20), Figure (21), Figure (22). The Shaft of the device was rotated from 0 to 90 degrees. Observations such as pressure drop, and flow rate were recorded and are shown in a tabular form below. Results from the experimental process are arranged in tabular form. Table (4), Table (5), and Table (6) show values recorded at starting Lpm of 0.6, 1 and 1.5. It was observed that when the FCD valve moves from 0^{o}-90^{o} of Angle the area of opening decreases and the pressure drop across the FCD increases which results in a reduction of the flow rate. This shows the impedance

characteristics of the FCD. A comparison of results from the experimental study and CFD analysis is shown in Figure (23), Figure (24) and Figure (25). The comparison of results of flow rates with varying angles of the ball valve shows that a maximum discrepancy of 20% was observed in both the results at a flow rate of 1 Lpm. This is expected as there is a linearly inverse relationship between pressure drop and flow rate. The maximum error between the pressure drop variation was 16% for at 1 Lpm flow rate when the valve is fully closed. The error between the results when the valve was fully opened was within 3% for both pressure drop and flow rate. The maximum value of pressure drops, and flow occurs between the angle of 30^{o} to 90^{o} angles.

At 0.6 Lpm @ fully open				
v=0.127 m/s	**Inlet Pressure (kPa)**	**Outlet pressure (kPa)**	**Flow Rate (Lpm)**	**Pressure drop in (kPa)**
Angle				
0	6.48	4.687	0.6	1.793
30	6.4375	4.125	0.559	2.3125
45	7.1875	3	0.366	4.1875
90	8.95	1.06	0	7.89

Table 4. Experimental Result showing increases in pressure drop with increase in damper angle at a Maximum of 0.6 Lpm.

At 1Lpm @ fully open				
v=0.2122 m/s	Inlet Pressure (kPa)	Outlet pressure (kPa)	Flow Rate (Lpm)	Pressure drop in (kPa)
Angle				
0	11.98	10.425	1.5296	2.023
30	12.456	9.125	0.865	5
45	16.979	4.005	0.512	13.63
90	18.563	2.663	0	16.57

Table 5. Experimental Result showing increases in pressure drop with increase in damper angle at Maximum of 1 Lpm.

At 1.5 Lpm @ fully open				
v=0.2122 m/s	Inlet Pressure (kPa)	Outlet pressure (kPa)	Flow Rate (Lpm)	Pressure drop in (kPa)
Angle				
0	22.5	19.5	1.5	3
30	24.5	17	1.35	7.5
45	29	7.5	0.814	21.5
90	34	1.375	0.103	32.625

Table 6.Experimental Result showing increases in pressure drop with increase in damper angle at a Maximum of 1.5 Lpm.

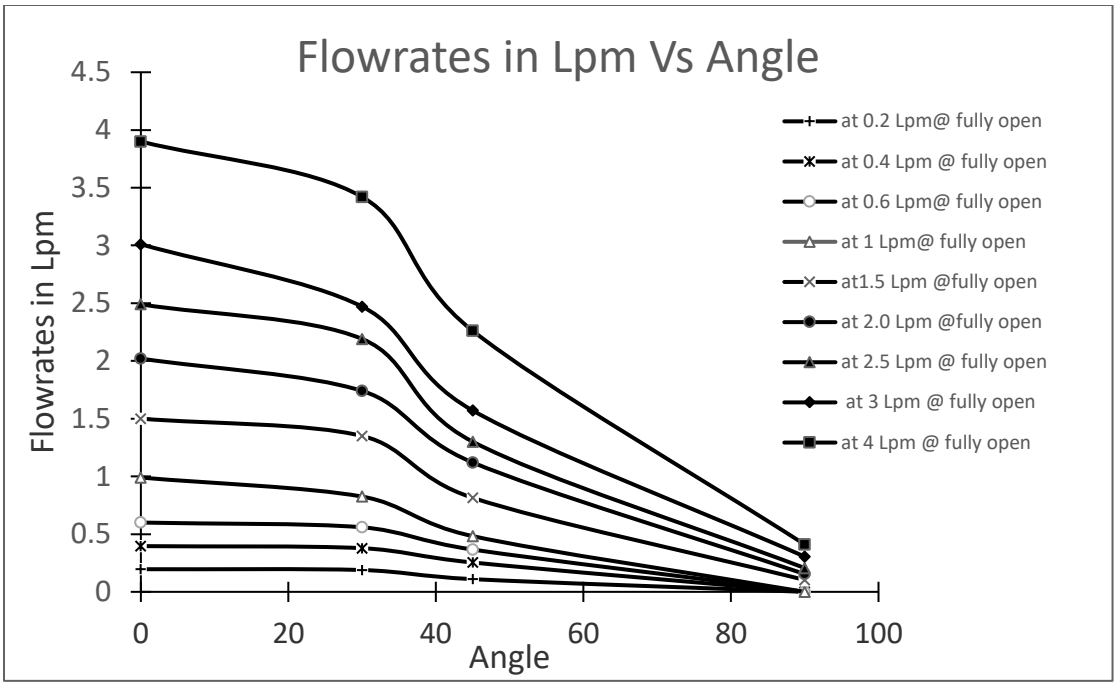

Figure 20. Variation of the flow rate through the FCD with the changing angle of the valve

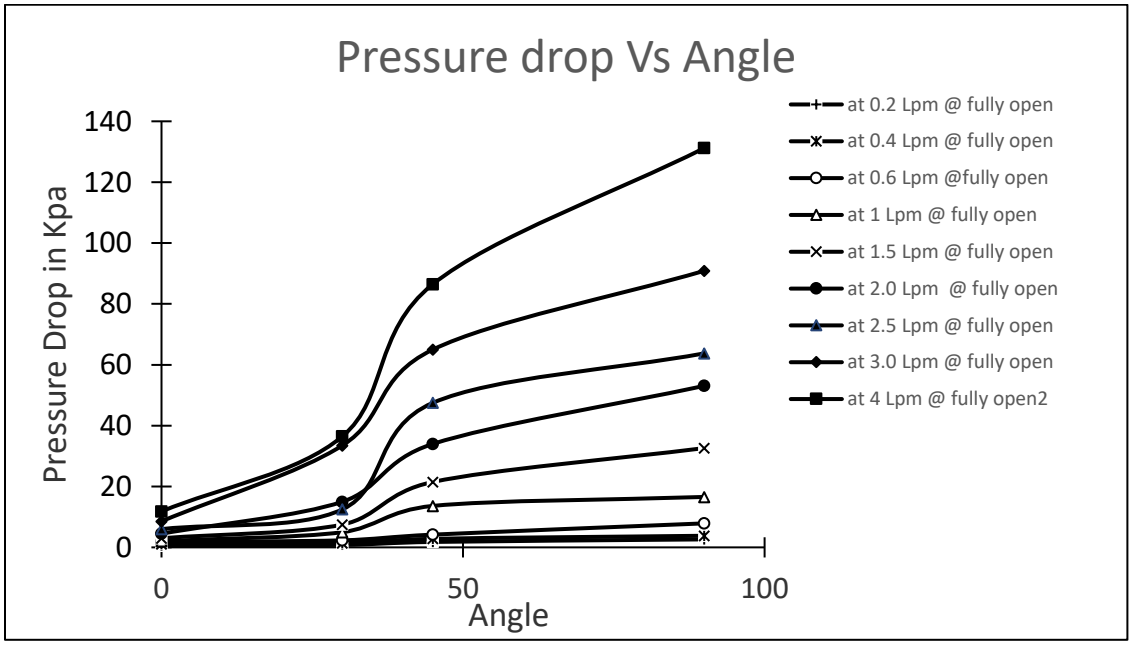

Figure 21. Pressure drop variation across the FCD with changing valve angle.

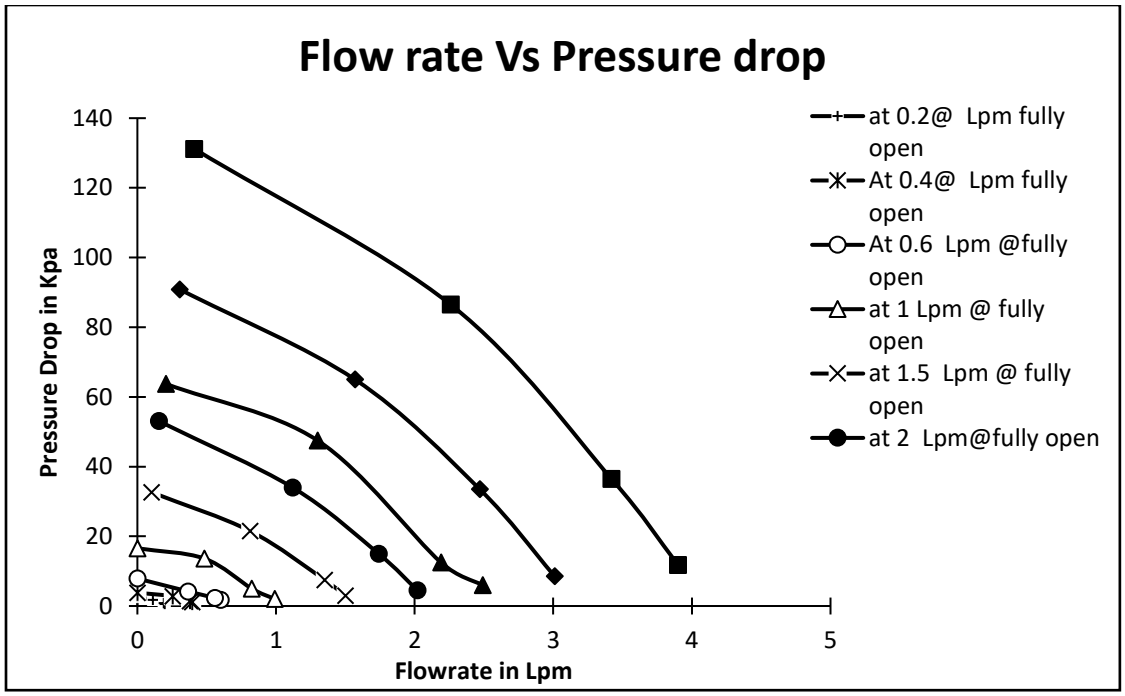

Figure 22. Device impedance curve with varying flow rates with the valve is in a fully open condition.

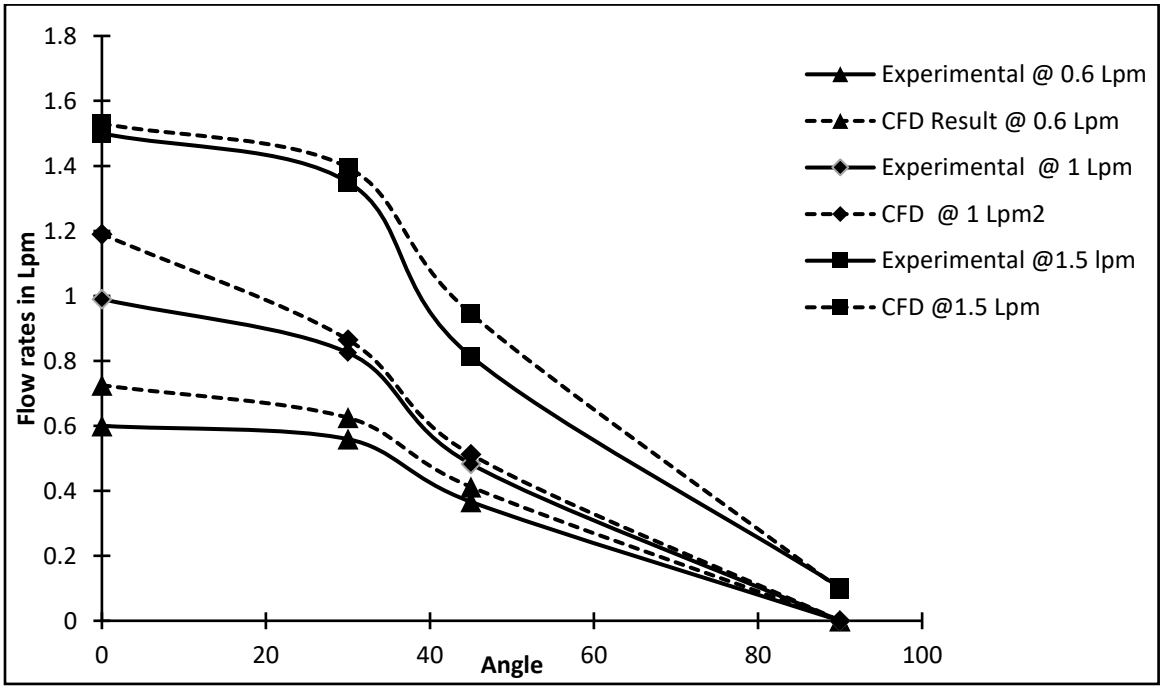

Figure 23. Variation of the flow rate through the FCD with the changing angle of the valve

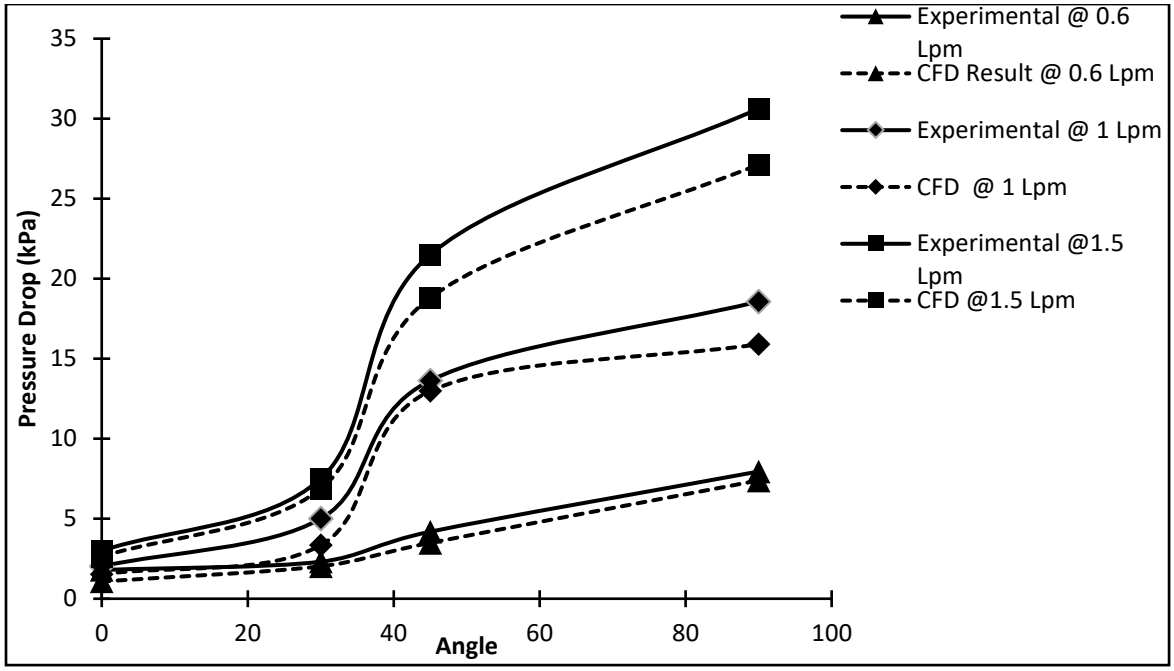

Figure 24. Pressure drop variation across the FCD with changing valve angle.

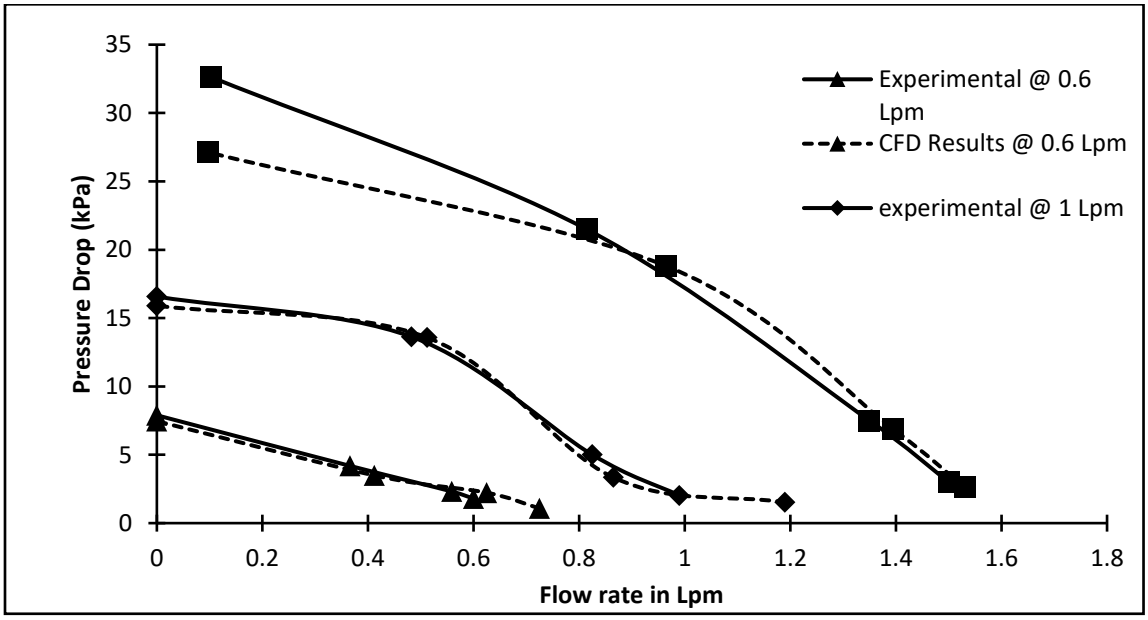

Figure 25. Comparison of the impedance curve obtained from CFD analysis and experimental data.

Chapter 5

Conclusion and Future work

Direct liquid cooling (DLC) has already proven to be an effective method in overcoming the thermal challenges faced in high-performance computation systems. The implementation of DLC has made the heat dissipation process more energy efficient for high heat flux components. DLC provides notable advantages and better equipment reliability of IT Equipment's as issues related to contamination and fan acoustics [29-34]. In traditional DLC datacenters, the coolant is supplied to the servers at a constant flow rate through a centralized pumping system irrespective of the utilization, but with the implementation of targeted coolant supply depending on the utilization of the server, further enhancement can be made in making the system more efficient. The targeted supply of coolant can be achieved using dynamic liquid cooling methods. Dynamic liquid cooling can be achieved by developing a control strategy that controls the pump speed, working simultaneously with a device that will obstruct the flow sullied to a particular load. It also provides higher heat flux values than single-phase immersion cooling and overcomes the issues related to material compatibility and vapor pressure in 2-phase open bath immersion cooling and 2-phase cold plates [35-40].

In our study, an FCD design is proposed, which will help in workload-related provisioning of the coolant to the servers placed in a data center. A recent study conducted by retrofitting cold plates with distributed pumps showed considerable power saving when the flow rates were dynamically varied [41]. The FCD will therefore yield a considerable power-saving when used simultaneously with speed control pumps on rack level. The V-cut ball valve design was finalized from the two designs by comparing their hydraulic characteristics. FEA analysis was conducted to find failure in the part. Various failure modes are caused by factors such as mechanical stresses,

temperature cycling, and humidity, making reliability a major concern. Finite element analysis (FEA) is commonly used to evaluate reliability under a variety of loading conditions, including thermal cycling, drop checking, power cycling, and vibrational loads [42]. The CFD analysis and the experimental validation shows that the FCD was efficient in providing the required variation in flow rates to cool heat loads in high powers computation systems. A minimum of 0.09 Lpm and a maximum of 4Lpm were achieved by varying the angle of the valve inside the FCD cavity.

The future work on this subject will investigate the implementation of FCD on servers at a rack level and obtain the thermal and hydraulic characteristics of the FCD when used on a rack level. In the future study, we will also investigate the pumping power saving achieved by the implementation of FCD on a rack level and the cost-saving not only due to reduced pumping power but also provide an estimate of a simple payback period after device deployment. Further studies will also focus on the reliability of the FCD at high cycle speeds to obtain the lifecycle when operated at transient conditions.

References

[1] Gao, T., Tang, H., Cui, Y., and Luo, Z., 2018, “A Test Study of Technology Cooling Loop in a Liquid Cooling System,” *17th IEEE Intersociety Conference on Thermal and Thermomechanical Phenomena in Electronic Systems (ITherm)*, San Diego, CA, 2018, pp. 740-747, doi: 10.1109/ITHERM.2018.8419519.

[2] Iyengar, M., 2010, “Energy Consumption of Information Technology Data Centers,”

J. Electron. Cool., 16(4), epub.

[3] Andy Lawrence, April 2020, “Data center PUEs flat since 2013”, Accessed January 7, 2020, Global Uptime Institute Survey, https://journal.uptimeinstitute.com/data-center-pues-flat-since-2013/

[4] Hoang, C.H., Khalili, S., Ramakrisnan, B., Rangarajan, S., Hadad, Y., Radmard, V., Sikka, K., Schiffres, S. and Sammakia, B., 2020, “An Experimental Apparatus for Two-phase Cooling of High Heat Flux Application using an Impinging Cold Plate and Dielectric Coolant,” *36th Semiconductor Thermal Measurement, Modeling & Management Symposium (SEMI-THERM)*, San Jose, CA, USA, 2020, pp. 32-38, doi: 10.23919/SEMI-THERM50369.2020.9142831.

[5] Shahi, P., Agarwal, S., Saini, S., Niazmand, A., Bansode, P., & Agonafer, D., 2020, "CFD Analysis on Liquid Cooled Cold Plate Using Copper Nanoparticles," Proceedings of the ASME 2020 International Technical Conference and Exhibition on Packaging and Integration of Electronic and Photonic Microsystems. ASME 2020 International Technical Conference and Exhibition on Packaging and Integration of Electronic and Photonic Microsystems. Virtual, Online. October 27–29,2020.V001T08A007. ASME. https://doi.org/10.1115/IPACK2020-2592

[6] Niazmand, A., Chauhan, T., Saini, S., Shahi, P., Bansode, P.V., & Agonafer, D., 2020, "CFD Simulation of Two-Phase Immersion Cooling Using FC-72 Dielectric Fluid." Proceedings of the ASME 2020 International Technical Conference and Exhibition on Packaging and Integration of Electronic and Photonic Microsystems. ASME 2020 International Technical Conference and Exhibition on Packaging and Integration of Electronic and Photonic Microsystems. Virtual, Online. October 27–29, 2020. V001T07A009. ASME. https://doi.org/10.1115/IPACK2020-2595

[7] Chu, R. C., Simons, R. E., Ellsworth, M. J., Schmidt, R. R., and Cozzolino, V., 2004, “Review of Cooling Technologies for Computer Products,” IEEE Trans. Device Mater. Reliab., 4(4), pp. 568–585.

[8] Ellsworth, M. J., Campbell, L. A., Simons, R. E., Iyengar, M. K., Schmidt, R. R., and Chu, R. C., 2008, “The Evolution of Water Cooling for Large IBM Large Server Systems: Back to the Future,” 11th Intersociety Conference on Thermal and Thermomechanical Phenomena in Electronic Systems (ITherm), Orlando, FL, May 28–31, pp. 266–274.

[9] McFarlane, R., 2012, “Will Water-Cooled Servers Make Another Splash in the Data Center?,” Tech Target Network, Search Data Center, Newton, MA, accessed Feb. 26, 2012,

https://searchdatacenter.techtarget.com/tip/Will-watercooled-servers-make-another-splash-in-the-data-center

[10] Schmidt, R. R., 2005, “Liquid Cooling Is Back,” Electronics Cooling, 11(3), (epub).

[11] Patrizio, A., 2018, “Lenovo Introduces New Water-Cooled Server Technology,” Network World, Framingham, MA, accessed Feb. 26, 2018, https://www.networkworld.com/article/3258646/data-center/lenovo-introduces-newwater-cooled-server-technology.html

[12] Koblentz, E., 2018, “How to Get Started With Liquid Cooling for Servers and Data Center Racks,” Data Centers Trends Newsletter, TechRepublic, US edition, accessed July 8, 2018, https://www.techrepublic.com/article/how-to-getstarted-with-liquid-cooling-for-servers-and-data-center-racks/

[13] Iyengar, M., David, M., Parida, P., Kamath, V., Kochuparambil, B., Graybill, D., Schultz, M., Gaynes, M., Simons, R., Schmidt, R., and Chainer, T., 2012, “Server Liquid Cooling With Chiller-Less Data Center Design to Enable Significant Energy Savings,” 28th Annual IEEE Semiconductor Thermal Measurement and Management Symposium (SEMI-THERM), San Jose, CA, Mar. 18–22, pp. 212–223.

[14] Fan, Y., Winkel, C., Kulkarni, D., and Tian, W., 2018, “Analytical Design Methodology for Liquid Based Cooling Solutions for High TDP CPUs,” 17th IEEE Intersociety Conference on Thermal and Thermomechanical Phenomena in Electronic Systems (ITherm), San Diego, CA, May 29–June 1, pp. 582–586.

[15] Gullbrand, J., Luckeroth, M. J., Sprenger, M. E., and Winkel, C. (March 1, 2019). "Liquid Cooling of Compute System." ASME. *J. Electron. Packag*. March 2019; 141(1): 010802. https://doi.org/10.1115/1.4042802

[16] Boucher, T. D., Auslander, D. M., Bash, C. E., Federspiel, C. C., and Patel, C. D. (November 11, 2005). "Viability of Dynamic Cooling Control in a Data Center Environment." ASME. *J. Electron. Packag*. June 2006; 128(2): 137–144. https://doi.org/10.1115/1.2165214

[17] Gandhi, Dynamic Server Provisioning for Data Center Power Management, pp. 1-174, June 2013.

[18] K. Hazelwood, S. Bird, D. Brooks, S. Chintala, U. Diril, D. Dzhulgakov, et al., "Applied Machine Learning at Facebook: A Datacenter Infrastructure Perspective", *IEEE International Symposium on High Performance Computer Architecture (HPCA)*, Vienna, 2018, pp. 620-629, doi: 10.1109/HPCA.2018.00059.

[19] V. K. Arghode, V. Sundaralingam and Y. Joshi, 2016, “Airflow Management in a Contained Cold Aisle Using Active Fan Tiles for Energy Efficient Data- Center Operation Airflow Management in a Contained Cold Aisle Using Active Fan Tiles for Energy Efficient Data-Center, Heat Transfer Engineering, 37:3-4, 246-256, DOI: 10.1080/01457632.2015.1051386

[20] S. Khalili, G. Mohsenian, A. Desu, K. Ghose and B. Sammakia, "Airflow Management Using Active Air Dampers in Presence of a Dynamic Workload in Data Centers," *35th Semiconductor Thermal Measurement, Modeling and Management Symposium (SEMI-THERM), San Jose, CA, USA, 2019, pp. 101-110.*.

[21] H. Xu, C. Feng and B. Li, "Temperature Aware Workload Management in Geo-Distributed Data Centers," in *IEEE Transactions on Parallel and Distributed Systems*, vol. 26, no. 6, pp. 1743-1753, 1 June 2015, doi:10.1109/TPDS.2014.2325836.

[22] Kasukurthy, Rajesh, 2019, "Design and Optimization of Energy Conserving Solutions in Data Center Application," PhD dissertation, The University of Texas at Arlington, Arlington, TX.

[23] Kasukurthy, R., Rachakonda, A., and Agonafer, D., November 6, 2020, "Design and Optimization of Control Strategy to Reduce Pumping Power in Dynamic Liquid Cooling," ASME. J. Electron. Packag. doi: https://doi.org/10.1115/1.4049018

[24] Tao, J., Lin, Z., Ma, C., Ye, J., Zhu, Z., Li, Y., and Mao, W. (October 30, 2019). "An Experimental and Numerical Study of Regulating Performance and Flow Loss in a V-Port Ball Valve," ASME. J. Fluids Eng. February 2020; 142(2): 021207. https://doi.org/10.1115/1.4044986

[25] Chern, M., and Wang, C. (July 12, 2004). "Control of Volumetric Flow-Rate of Ball Valve Using V-Port ." ASME. J. Fluids Eng. May 2004; 126(3): 471–481. https://doi.org/10.1115/1.1760536

[26] Ansys® FLUENT, Release 2019R3, ANSYS Fluent User's Guide, [book and chapter reference name/numbers], ANSYS, Inc.

[27] Blazek, J., 2015. *Computational fluid dynamics: principles and applications*. Butterworth-Heinemann.

[28] Lin, F. and Schohl, G.A., 2004, "CFD prediction and validation of butterfly valve hydrodynamic forces," World Water and Environmental Resources Congress 2004

June 27-July 1, 2004, Salt Lake City, Utah, pp. 1-8 https://doi.org/10.1061/40737(2004)232

[29] Shah, J.M., Anand, R., Saini, S., Cyriac, R., Agonafer, D., Singh, P., & Kaler, M., 2019, "Development of a Technique to Measure Deliquescent Relative Humidity of Particulate Contaminants and Determination of the Operating Relative Humidity of a Data Center, " Proceedings of the ASME 2019 International Technical Conference and Exhibition on Packaging and Integration of Electronic and Photonic Microsystems. ASME 2019 International Technical Conference and Exhibition on Packaging and Integration of Electronic and Photonic Microsystems. Anaheim, California, USA. October 7–9, 2019. V001T02A016. ASME. https://doi.org/10.1115/IPACK2019-6601

[30] Saini, Satyam, 2018, “Airflow Path and Flow Pattern Analysis of Sub-Micron Particulate Contaminants in a Data Center with Hot Aisle Containment System Utilizing Direct Air Cooling,” The University of Texas at Arlington, Arlington, TX.

[31] Saini, S., Shahi, P., Bansode, P., Siddarth, A., Agonafer, D., 2020, "CFD Investigation of Dispersion of Airborne Particulate Contaminants in a Raised Floor Data Center," 36th Semiconductor Thermal Measurement, Modeling & Management Symposium (SEMI-THERM), San Jose, CA, USA, 2020, pp. 39-47, doi: 10.23919/SEMITHERM50369.2020.9142865.

[32] Thirunavakkarasu, G., Saini, S., Shah, J.M., Agonafer, D., 2018, "Air Flow Pattern and Path Flow Simulation of Airborne Particulate Contaminants in a High-Density Data Center Utilizing Airside Economization," Proceedings of the ASME 2018 International Technical Conference and Exhibition on Packaging and Integration of Electronic and Photonic Microsystems. ASME 2018 International Technical Conference and Exhibition on Packaging and Integration of Electronic and Photonic Microsystems. San Francisco, California, USA. August 27–30, 2018. V001T02A011. ASME. https://doi.org/10.1115/IPACK2018-8436

[33] Saini, S., Adsul, K.K., Shahi, P., Niazmand, A., Bansode, P., & Agonafer, D., 2020, "CFD Modeling of the Distribution of Airborne Particulate Contaminants Inside Data Center Hardware," Proceedings of the ASME 2020 International Technical Conference and Exhibition on Packaging and Integration of Electronic and Photonic Microsystems. ASME 2020 International Technical Conference and Exhibition on Packaging and Integration of Electronic and Photonic Microsystems. Virtual, Online. October 27–29, 2020. V001T08A005. ASME. https://doi.org/10.1115/IPACK2020-2590

[34] Shah, J. M., Anand, R., Singh, P., Saini, S., Cyriac, R., Agonafer, D., and Kaler, M. (June 23, 2020). "Development of a Precise and Cost-Effective Technique to Measure Deliquescent Relative Humidity of Particulate Contaminants and Determination of the Operating Relative Humidity of a Data Center Utilizing Airside Economization." ASME. J. Electron. Packag. December 2020; 142(4): 041103. https://doi.org/10.1115/1.4047469

[35] Gandhi, D., Chowdhury, U., Chauhan, T., Bansode, P.V., Saini., S, Shah, J.M., & Agonafer, D., 2019, "Computational Analysis for Thermal Optimization of Server for Single Phase Immersion Cooling," Proceedings of the ASME 2019 International Technical Conference and Exhibition on Packaging and Integration of Electronic and Photonic Microsystems. ASME 2019 International Technical Conference and Exhibition on Packaging and Integration of Electronic and Photonic Microsystems. Anaheim, California, USA. October 7–9, 2019. V001T02A013. ASME. https://doi.org/10.1115/IPACK2019-6587

[36] Shinde, P.A., Bansode, P.V., Saini, S., Kasukurthy, R., Chauhan, T., Shah, J.M., & Agonafer, D., 2019, "Experimental Analysis for Optimization of Thermal Performance of a Server in Single Phase Immersion Cooling," Proceedings of the ASME 2019 International Technical Conference and Exhibition on Packaging and Integration of Electronic and Photonic Microsystems. ASME 2019 International Technical Conference and Exhibition on Packaging and Integration of Electronic and Photonic Microsystems. Anaheim, California, USA. October 7–9, 2019. V001T02A014. ASME. https://doi.org/10.1115/IPACK2019-6590

[37] Bansode, P. V., Shah, J. M., Gupta, G., Agonafer, D., Patel, H., Roe, D., and Tufty, R. (November 8, 2019). "Measurement of the Thermal Performance of a Custom-Build Single-Phase Immersion Cooled Server at Various High and Low Temperatures for Prolonged Time." ASME. *J. Electron. Packag*. March 2020; 142(1): 011010. https://doi.org/10.1115/1.4045156

[38] Niazmand, A., Murthy, P., Saini, S., Shahi, P., Bansode, P., & Agonafer, D., 2020, "Numerical Analysis of Oil Immersion Cooling of a Server Using Mineral Oil and Al2O3 Nanofluid," Proceedings of the ASME 2020 International Technical Conference and Exhibition on Packaging and Integration of Electronic and Photonic Microsystems. ASME 2020 International Technical Conference and Exhibition on Packaging and Integration of Electronic and Photonic Microsystems. Virtual, Online. October 27–29, 2020. V001T08A009. ASME. https://doi.org/10.1115/IPACK2020-2662

[39] Kumar, A., Shahi, P., Saha, S.K., 2018, "Experimental study of latent heat thermal energy storage system for medium temperature solar applications," In Proceedings of the 4th World Congress on Mechanical, Chemical, and Material Engineering (MCM'18), Madrid, Spain, pp. 16-18.

[40] Hoang, C.H., Khalili, S., Ramakrisnan, B., Rangarajan, S., Hadad, Y., Radmard, V., Sikka, K., Schiffres, S. and Sammakia, B., 2020, March, "An Experimental Apparatus for Two-phase Cooling of High Heat Flux Application using an Impinging Cold Plate and Dielectric Coolant," In *2020 36th Semiconductor Thermal Measurement, Modeling & Management Symposium (SEMI-THERM)*, pp. 32-38, doi: 10.23919/SEMI-THERM50369.2020.9142831.

[41] Shahi, P., Saini, S., Bansode, P., and Agonafer, D., 2021, "A Comparative Study of Energy Savings in a Liquid-Cooled Server by Dynamic Control of Coolant Flow Rate at Server Level," in IEEE Transactions on Components, Packaging and Manufacturing Technology, 11(4), pp. 616-624, doi: 10.1109/TCPMT.2021.3067045.

[42]A. Lakshminarayana, A. Misrak, R. Bhandari, T. Chauhan, A. S. M. R. Chowdhury, and D. Agonafer, "Impact of Viscoelastic Properties of Low Loss Printed Circuit Boards (PCBs) on Reliability of WCSP Packages Under Drop Test," in *2020 IEEE 70th Electronic Components and Technology Conference (ECTC)*, 2020, pp. 2266–2271, doi:10.1109/ECTC32862.2020.00353.

[43] Shahi, P., Deshmukh, A.P., Hurnekar, H.Y., Saini, S., Bansode, P., Kasukurthy, R., Agonafer, D., 2021, "Design, Development and Characterization of a Flow Control Device for Dynamic Cooling Liquid Cooled Servers," ASME Journal of Electronic Packaging.

Illustration Reference

[44] Pitayachaval, P. and Kriengsak Masnok. "Feed rate and volume of material effects in fused deposition modeling nozzle wear." *2017 4th International Conference on Industrial Engineering and Applications (ICIEA)* (2017): 39-44.